OPTIMIZATION OF FAN NOISE BY COUPLING 3D INVERSE DESIGN AND AUTOMATIC OPTIMIZER

Mehrdad ZANGENEH[1], Matthieu DE MAILLARD[2]

[1] Department of Mechanical Engineering, University College London, Torrington Place, London, WC1E 7JE, UK.

[2]Advanced Design Technology Ltd, Dilke House, 1 Malet Street, London WC1E 7JN

SUMMARY

In many electronic cooling applications there is in increasing demand for high pressure rise compact axial fan design. This can only be achieved by increasing fan rpm, which can result in higher noise. In this paper a methodology is presented based on coupling a 3D inverse design method together with Design of Experiments, Response Surface modeling and Multi-objective Genetic algorithms in order to improve the efficiency and tonal noise from high rpm cooling fans.

INTRODUCTION

In many electronic cooling applications axial fans are coupled directly with heat sinks and this has resulted in requirements for relatively high fan pressure rise and compact size, see [1]. This type of design can only be achieved by using higher fan rpm, which may result in substantial increase in fan noise, especially tonal noise. At the same time in many fan applications, especially in datacenters, there is a need for improving fan efficiency. The requirements on noise and efficiency of axial fans pose a difficult multi-objective problem for 3D design of axial fans.

Axial fans are conventionally designed by an iterative (direct) approach, which starts from an assumed blade shape whose performance is evaluated by CFD codes, see for example [2]. However, since the flow field is highly complex and 3D and there is no direct relationship between the blade geometry and flow field, the design process has to rely on experience of designers. Generally speaking experienced designers can achieve good designs by following closely what has worked in the past. However, such an approach can, inadvertently, result in a reduction of the design space as the designer tends to operate within his comfort zone. Hence using this approach will make it more difficult to achieve designs beyond previous experience (e.g higher pressure rise) or designs that meet constrasting multi-objective requirements on noise and efficiency.

An alternative method for aerodynamic design of fan blades is the inverse design approach, in which the blade geometry is computed for a specified distribution of blade loading. Since the blade loading is directly related to the pressure difference across the blade, the method allows the designer to directly control the 3-D pressure field in the fan and hence have a direct control over the viscous flow field. This approach removes the need for empiricism in the design process and allows designers to more directly explore a larger part of the design space.

A 3D inverse design code that has already been applied to many axial fan applications is TURBOdesign1 [3]. In this inverse design method the blade geometry is computed for a specified distribution of blade loading ($\partial r\overline{V}_\theta / \partial m$), which is the meridional derivative of the tangentially mean swirl velocity and is directly related to the blade bound circulation $2\pi r\overline{V}_\theta$. In this method, in addition to the blade loading the normal thickness distribution is specified and hence it is possible to ensure structural integrity of the design. The method has already been applied to improve aerodynamic performance of axial fans and reduce broadband noise and improve efficiency, see [4], [5] and [6].

In this paper the inverse design code TURBOdesign1 will be used together with an automatic optimization platform TURBOdesign optima [7] and a tonal noise model based on Ffowcs-William Hawkins approach [8] to optimize the noise and efficiency of a generic high pressure rise axial cooling fan.

DESCRIPTION OF THE DESIGN STRATEGY

The Optimization Process

TURBOdesign Optima [7], provides a platform for different optimization strategies based on inputs to 3D inverse design code TURBOdesign1. In this study, Workflow 4 which couples Design of Experiments Method, Response Surface Modeling and Multi-objective Genetic Algorithm was used.

Generally speaking, a design process can be considered as the optimization of the functions correlating the performance parameters P_j to the design factors X_i:

$$P_j = P_j(X_i) \qquad i = 1, N \quad j = 1, M \tag{1}$$

In the case of an aerodynamic design, the exact value of these functions is given by an aerodynamic analysis, like a CFD evaluation.

In the engineering design, statistical techniques have been widely used in order to build approximations of these functions. In the present work, the Response Surface Methodology (Myers [9]) coupled with the Design of Experiments (DOE) technique (Taguchi [10]) was applied.

The RSM approximates the objective functions with polynomials (response surfaces), whose order and shape must be chosen beforehand. In common practice, a first- or second-order polynomial function is usually used:

$$P_j = \beta_0^j + \sum_{i=0}^{n} \beta_i^j X_i + \sum_{i=0}^{n} \beta_{ii}^j X_i^2 + \sum_{i \neq j}^{n} \beta_{ik}^j X_i X_k \tag{2}$$

The polynomial coefficients β_0, β_i, β_{ii} and β_{ij} are determined by means of a standard least-square regression which minimizes the sum of the square of the deviations of the predicted values from the actual ones for a set of points. The DOE theory provides the sampling points, at which to perform the tests, in order to minimize the necessary number of simulations.

The validity of the model is verified through the analysis of two parameters: R^2 (the ratio of the model sum of squares to the total sum of squares) and R^2_{adj} (R^2 adjusted to the number of parameters in the model).

From the analysis of the approximated model, it is possible to quantify the impact of each design parameter (coefficients β_i and β_{ii}) and the effect of their interactions (coefficients β_{ij}).

After all the models have been created, a multi-objective genetic algorithm [11] is applied to the obtained response functions. As a result, the Pareto front of the optimal solutions is determined. Then, depending on the design specifications, the best compromise between different performance parameters is chosen on the Pareto front.

Blade Parameterization

The commercial software TURBOdesign1 is used to parametrically describe the blade geometry. TURBOdesign1 (see [12]) is a three-dimensional inviscid inverse design method, where the distribution of the circumferentially averaged swirl velocity (rV_θ) is prescribed on the meridional channel of the blade and the corresponding blade shape is computed iteratively.

The circulation distribution is specified by imposing the spanwiser V_θ distribution at leading and trailing edge and the meridional derivative of the circulation drV_θ/dm (blade loading) inside the blade channel. The input design parameters required by the program are the following:

- Meridional channel shape in terms of hub, shroud, leading and trailing edge contours.
- Normal/tangential thickness distribution.
- Fluid properties and design specifications.
- Inlet flow conditions in terms of spanwise distributions of total temperature and velocity components.
- Exit rV_θ spanwise distribution. By controlling its value, the work coefficient (rotor) or flow turning (stator) are controlled.
- Blade loading distribution (drV_θ/dm). It is imposed at two or more span locations. The code then automatically interpolates span-wise to obtain the two-dimensional distribution over the meridional channel.
- Stacking condition. The stacking condition must be imposed at a chord-wise location between leading and trailing edge. Everywhere else the blade is free to adjust itself according to the loading specifications.

Noise Model

The aeroacoustics model used in this study is based on the Farassat's 1A formulation of the Ffowcs-Williams Hawkins method [7]. The details of a similar numerical implementation of this methodology and its validation against experimental data is presented in [13]. In this study only the solid wall model of the formulation was used as the flow in the fan can be considered as low subsonic flow. Hence the quadruple terms in the FWH model were neglected and the two terms considered where the so-called thickness noise $P'_T(x,t)$ and loading noise $P'_L(x,t)$. For a stationary observer these terms can be expressed as:

Thickness Noise:

$$4\pi p'_T(x,t) = \int_{f=0} \left[\frac{\rho_0 (v_n + v_n)}{r \; |1-M_r|^2} \right]_{ret} dS + \int_{f=0} \left[\frac{\rho_0 v_n (rM_i r_i + c_0 M_r - c_0 M^2)}{r^2 (1-M_r)^3} \right]_{ret} dS \qquad (3)$$

where r is the source-to-observer distance, ρ_0 is the undisturbed fluid density and c_0 the speed of sound. **M** of magnitude M is the Mach number vector of a source point on the blade surface S, which moves with an outward normal velocity v_n. The dotted quantities denote time derivative with respect to the emission time τ. M_r is the relative Mach number, i.e., the projection of **M** in the observer's direction.

Loading Noise:

$$4\pi p'_L(x,t) = \frac{1}{c_0} \int_{f=0} \left[\frac{\cdot l_i r_i}{r(1-M_r)^2} \right]_{ret} dS + \int_{f=0} \left[\frac{l_r - l_i M_i}{r^2 (1-M_r)^2} \right]_{ret} dS + \frac{1}{c_0} \int_{f=0} \left[\frac{l_r (rM_i r_i + c_0 M_r - c_0 M^2)}{r^2 (1-M_r)^3} \right]_{ret} dS \qquad (4)$$

where the rate of change of force vector in the blade-fixed co-ordinate is given by

where ω_t is the rotational velocity and is the unit outward normal vector to the blade surface with components . In this study we will only use steady blade surface pressure to compute the pressure force and hence is zero. The blade surface pressure is actually obtained from 3D inverse design code TURBOdesign1. The code is inviscid but provides a fairly accurate prediction of the surface static pressure on the blade. A comparison of the surface static pressure from CFD results and from TURBOdesign1 for the baseline fan is shown in Fig. 1. This approach has already been verified experimentally for a similar fan rotor and the method can predict the measured noise in the fan with high level of accuracy.

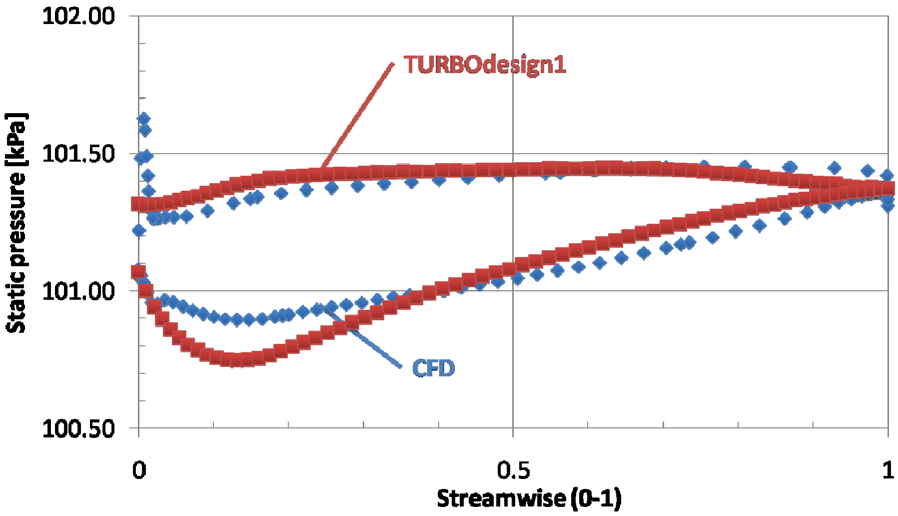

Figure 1: Comparison of surface static pressure between TURBOdesign1 and CFD

The total pressure fluctuation in time domain can then obtained by summing the contribution from the terms in equations 3 and 4, i.e.

Fast Fourier Transform is then used to convert the time domain data to frequency domain.

Baseline Fan Rotor

The baseline fan rotor is a generic fan design set up for this study with main geometrical features shown in table 1 and with two main duty points shown in table 2.The baseline rotor was generated by 3D inverse design code TURBOdesign1. In this code, the rotational speed, the design flow rate, the number of blades, and the meridional geometry have to be specified. In this study, no attempt was made to re-design the meridional geometry, and a rotor with constant hub and shroud radius and constant axial chord from hub to shroud was used. The design flow rate used in the code was at 1.434 m^3/min, which is almost half way between the two specified duty points. Once the basic design parameters and the meridional geometry are fixed, three additional input specifications, i.e. the spanwise$r\bar{V}_\theta$, the blade loading($\partial r\bar{V}_\theta / \partial m$)and the stacking conditions need to be specified. The average value of spanwise $r\bar{V}_\theta$ is directly related to the pressure rise at the design point but its spanwise variation essentially affects the circulation distribution on the blade and is an important design parameter. The meridional derivative of $r\bar{V}_\theta$is directly related to the pressure jump across the blade at each streamline and hence its used to control the blade surface pressure distribution. The blade loading was controlled by specifying the distribution of $\partial r\bar{V}_\theta / \partial m$ on the hub and shroud sections. Both distributions were parameterized by means of the three-segment method, which employs a combination of two parabolic curves and an intermediate linear line. Four parameters are required to control each distribution (see Fig.2):

- NC: intersection between the first parabolic distribution and the linear segment.
- ND: intersection between the linear segment and the second parabola.
- SLOPE: slope of the linear line. This parameter controls the loading distribution type: a positive value leads to a fore-loaded distribution, a negative one leads to an aft-loaded distribution.
- DRVT: blade loading at the leading edge. This parameter controls the flow incidence and then the inlet blade angle. If set to zero, a zero-incidence condition is imposed.

For the baseline design the free vortex spanwise$r\bar{V}_\theta$was used in which the same value of $r\bar{V}_\theta$was specified across the span. The blade loading specified for the baseline design is shown in Fig. 3. The baseline rotor was designed with zero incidence and a mid-loaded distribution (Fig. 3).

As far as the stacking condition is concerned, the wrap angle (i.e. θ–values of the camberline) distribution is specified along a single quasi-orthogonal line from the hub to the shroud. The stacking condition can affect the blade sweep and can have a significant effect on the 3D pressure field in the fan. For the baseline design, constant stacking with zero values of wrap angle was applied at the trailing edge plane. The thickness chosen is a NACA 0012 profile. The fan is an unshrouded impeller with 5 blades and a tip gap of 0.5mm.

Table 1: Geometrical data

	Baseline
Hub radius	19mm
Shroud Radius	30mm
Blade Number	5
Tip Gap	0.5mm

Table 2: Key duty points for baseline rotor

	RPM	Flow Rate (m^3/min)	Pressure Rise (Pa)
Duty Point 1	12000	1.2	>190
Duty Point 3	12000	1.6	>290

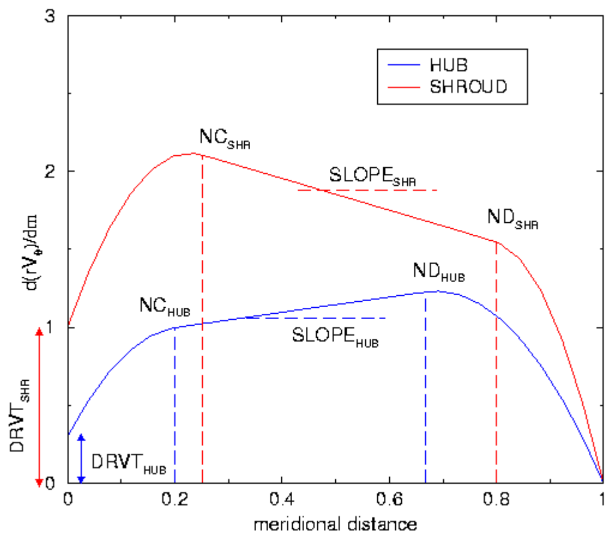

Figure 2: Blade loading paramertrization

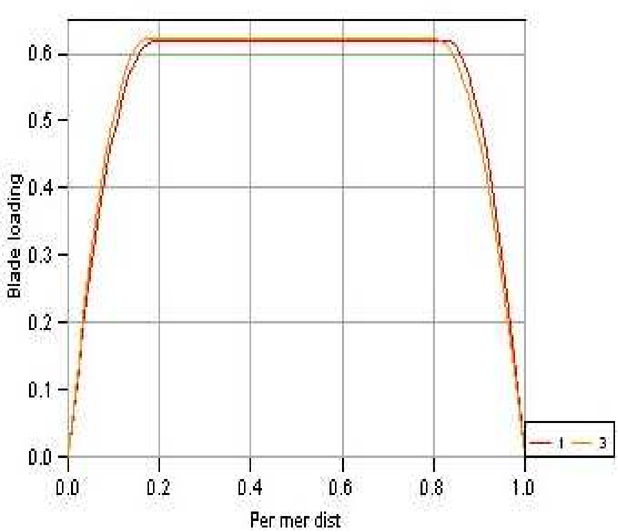

Figure 3: Blade loading of the baseline rotor

Optimization Target and Design Parameterization

The goalof this analysis is to study the effectof some of the major aerodynamicand geometrical parameters on the fan design point noise and duty point aerodynamic performance.The following performanceparameters were considered:

- Total to Total Efficiency of the rotor at duty points 1 and 2.
- Total-Static pressure rise in the rotor at duty points 1 and 2
- Tonal noise as computed by equations 3 and 4 at the design point.

For design parameters the following parameters were varied;

- Blade loading
- Stacking
- Spanwise

For blade loading the values of NC and ND at the hub and shroud were kept fixed but the values of Slope at the hub and shroud and DRVT at leading edge at the hub and shroud were varied. In all optimization problem the correct of choice of range of variation of design parameters is an important part of setting up the problem. By using inverse design based optimization the correct choice of parameters can be visually explored with ease. In this case the range was varied as shown in Table 3.

Table 3 – Range of variation of loading parameters

$SLOPE_{SHR}$ & $SLOPE_{HUB}$	-1.5 to 1.5
$DRVT_{SHR}$ & $DRVT_{HUB}$	0 to 0.9

The effect of these changes in blade loading parameters are shown in Fig. 4. The red line has been set to DRVT = 0.9 and SLOPE = -1.5 while the orange line has been set to DRVT = 0.0 and SLOPE = 1.5. The DoE method in fact automatically varies the range of parameters between these extreme limits. So in total 4 design parameters were used to control the blade loading.

The spanwise was varied linearly from hub to shroud. The mean value was kept constant at 0.452 m^2/s to ensure that all designs provide the correct level of pressure rise but the distribution was varied by + and – 20% of this value at the hub and shroud. This was done by just varying the shroud value and computing the hub value from the fixed mean value of . So in fact only one design parameter was used to control the spanwise .

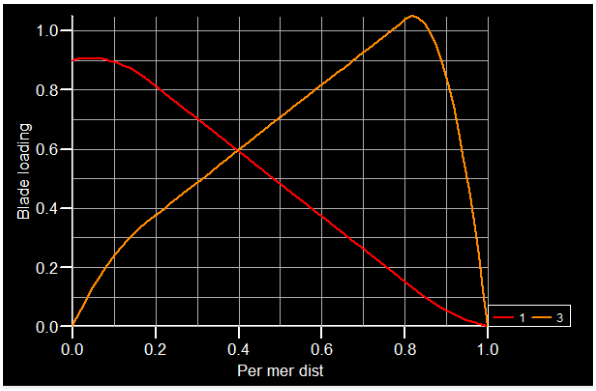

Figure 4 Range of variation of loading parameters used for optimization

Finally the stacking value and its position was varied. The stacking position was varied from 60% of axial chord to trailing edge and the value of wrap angle at the stacking location was varied from -10 degree to +10 degrees. So overall 7 design parameters were used in total.

Design Strategy and Computational Details

The purpose of this study is to investigate the influence of design parameters on noise and aerodynamic performance. The analysis was performed using a quadratic response surface where all the interactions were taken into account. In order to create the response function the DOE theory was used to create an experimental table, which consisted of 36 configurations. For each configuration to be analyzed, CFD calculations were carried out for the duty points (see Table 2) and the design point in order to describe the characteristic.

All geometries were analysed by using the 3D CFD code ANSYS CFX 12.1. Steady and incompressible flow calculationswere carried out for all of the cases. A high resolution for the advection scheme, a first order numeric option for the turbulence and an auto timescale have been chosen.To limit the boundary condition influence on the fan efficiency and also to comply with AMCA requirements, big domains have been created for the inlet and outlet with the following dimensions (see Figure 5):

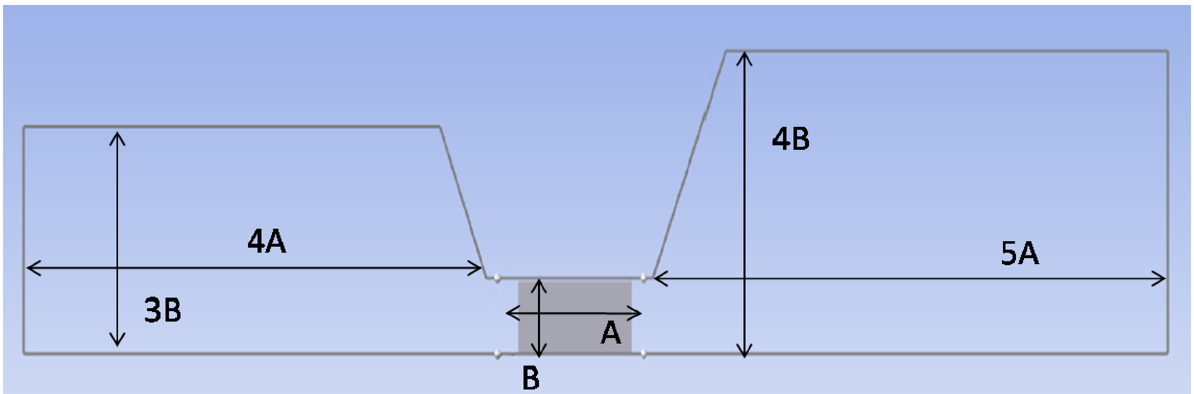

Figure 5: Computational domain used for CFD

The inlet domain, the outlet domain and the passage are about 120k nodes each, which makes a total of 360k nodes.The same mesh topology (H-O Grid) was used for all the design cases with 196 streamwise nodes (46 in the blade region), 50 spanwise nodes (with 8 in the tip clearance of 0.5 mm) and 28 blade-to-blade flow passage. For each computation the outlet was an opening with a fixed static pressure and flow direction, whereas the inlet was given a mass flow rate which changed for the different points. A standard k-ε model was used for all the cases. A frozen rotor was used between the inlet, outlet domains and the blade region. In general the value of Y^+ was between 8 and 10 and never went above 20. A typical computational mesh used is shown in Fig. 6.

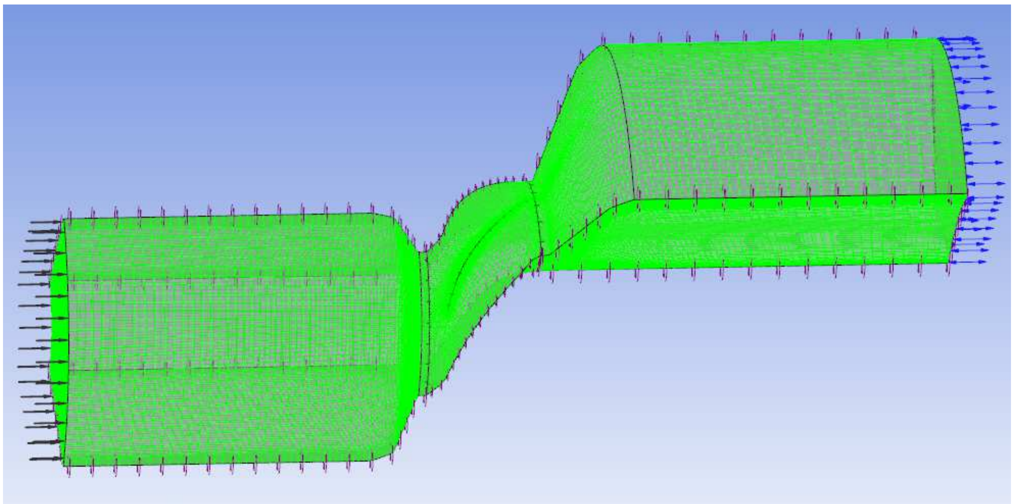

Figure 6: Typical computational mesh used for CFD

The blade surface static pressure and geometry of each of the 36 rotors were passed to the tonal noise model code and this was used to compute the resulting noise for each rotor. The example of a typical result for the total noise (sum of the thickness and loading noise) at a location about 1m upstream of the fan centre line, is shown in Fig. 7 for the baseline rotor. The predicted noise level at this location of 1 m upstream of fan centerline was at 1 kHz frequency was computed for all the 36 different geometries and used for optimization.

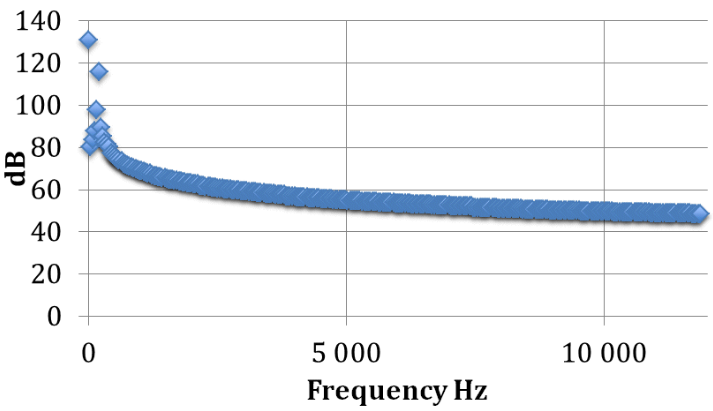

Figure 7: The noise prediction for the baseline rotor

ANALYSIS OF THE OPTIMIZATION RESULTS

The computed CFD results for each of the 36 configuration is then used to create the final design matrix. The data is then used in the Response Surface Method to create the response surface. The accuracy of the response surface is first checked by using the R^2value which is found to be 99% confirming a very high degree of accuracy for the response surface. The response surface can then be used for sensitivity analysis, showing the variation of important performance parameters with different design parameters. An example of this is shown in Fig. 8. The sensitivity analysis shows immediately that some parameters have more important effect on performance parameters than others. For example the tonal noise is more directly affected by Stacking Position, $DRVT_{HUB}$, and $SLOPE_{HUB}$. Efficiency at low flow rate (Duty point 1) is actually affected by $SLOPE_{HUB}$, Stacking value and value of spanwise at the shroud. One interesting aspect of the results to note is that in the values of $SLOPE_{HUB}$ or stacking at the hub that results in high efficiency at low flow rate in factresults in high noise and hence there is a clear trade-off between noise and efficiency at low flow rate.

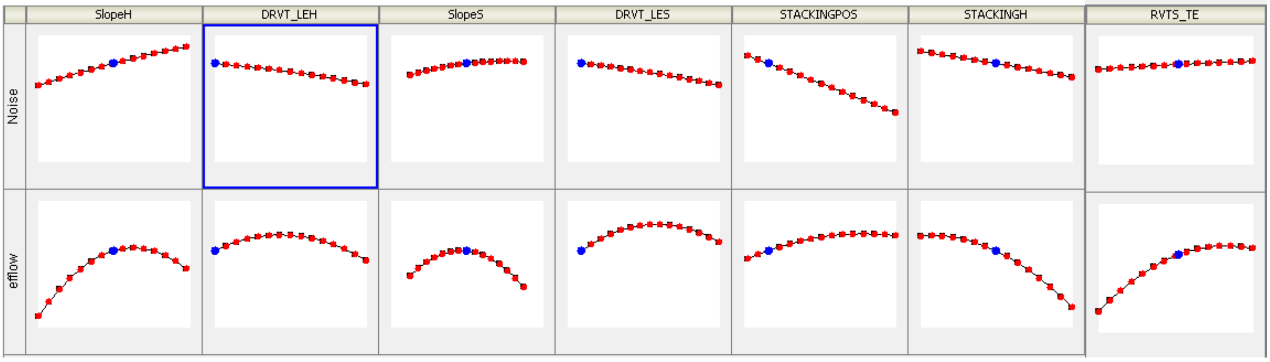

Figure8 – Results of Sensitivity analysis showing the variation of Tonal Noise and Efficiency at Low Flow with the 7 design parameters.

MOGA and Pareto Front

In order to find the best compromise solution between minimum tonal noise and maximum efficiency at low flow, a Multi-objective Genetic Algorithm (MOGA) was run on the Response Surface. For the MOGA, NSGA-II was used as described above. For this purpose an initial population of 80 and 80 generations were used resulting in a total population size of 6400. The same 7 design parameters and range of variation of these parameters as the DoE table were used.

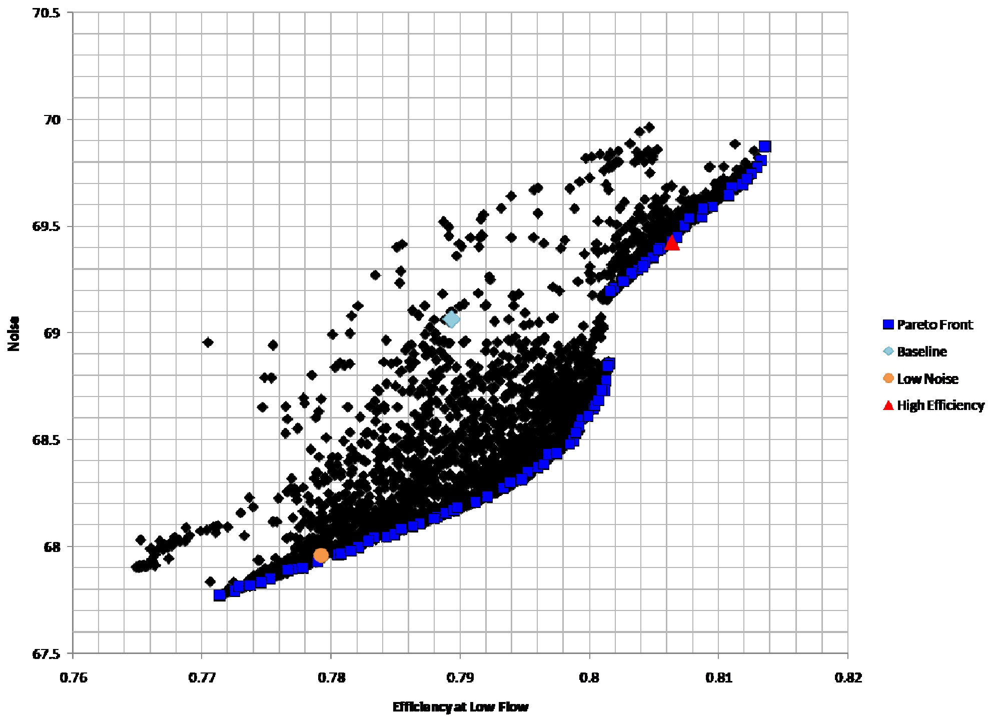

Figure 9: MOGA results and Pareto Front

The main performance parameters were the efficiency at low flow and the tonal noise. As objective the efficiency was maximized and the tonal noise minimized. A constraint was also used on the minimum pressure rise at low flow rate of greater than 290 Pa. The advantage of running the MOGA on the response surface is that the performance parameters for the 6400 different geometries created by the MOGA can be obtained in a matter of minutes by using the response surface method. The results of the optimization is summarized in Fig. 9, where the vertical axis shows the noise and the horizontal axis the efficiency at low flow (duty point 1) for all the 6400 geometries. The design space results in almost 2.5 dB variation in noise and 4 point variation in efficiency at low flow.The Pareto Front is shown in blue and it represents the best possible compromise solution between noise and efficiency over the selected design space, set by the number and range of design parameters used for DoE and optimization. In this figure the results of the CFD analysis and tonal noise analysis for the baseline rotor have been shown as a light blue point. Clearly the baseline design is well away from Pareto Optimal line.

Two points on the Pareto Optimal line were selected for analysis; one at low noise and the other at high efficiency end of the Pareto Front.These are indicated by orange circle and red triangle on the Pareto Front.For the High Efficiency case the $r\bar{V}_\theta$at the trailing edge varied from 0.35 m^2/s at the hub to 0.554 m^2/s at the shroud while for the Low Noise case it is 0.4m^2/s at the hub to 0.51m^2/s at the shroud.The stacking condition for the Low Noise design is 7.84° at the trailing edge and for the High Efficiency design it is -9.2°at 78% of axial chord. The blade loading for High Efficiency design has a fore-loaded distribution at the shroud and an aft-loaded distribution at the hub, as shown in Fig. 10. However, the blade loading for the Low Noise design is fore-loaded both at the hub and shroud as shown in Fig. 10. The geometry of the two designs from the Pareto front and the baseline are compared in Fig. 11.

The performance of the two designs from the Pareto Front (High Efficiency and Low Noise) were analyzed by using CFX. Furthermore, the noise computations were performed on these two geometries. In table 4 and 5 the results from actual CFD/Noise computations and the data obtained from Response Surface are compared. The results show that generally the response surface has accurately predicted the noise and efficiency level.

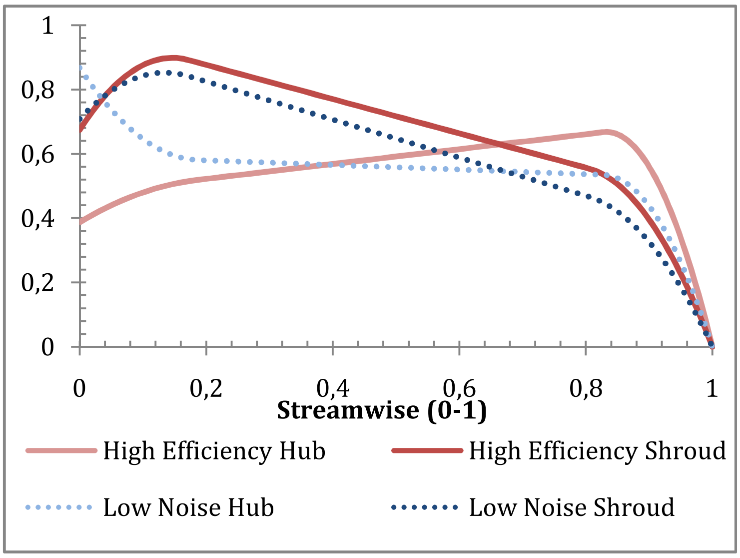

Figure10: Comparison of blade loading

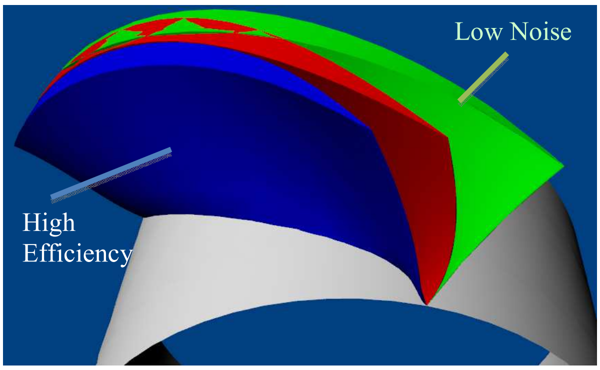

Figure 11: Geometrical comparison at the shroud

Table 4 – Actual versus RSM values for efficiency at low flow

	High Efficiency	Low Noise
Efficiency – CFD	0.8	0.778
Efficiency –RSM	0.804	0.779
% error	0.60%	0.12%

Table 5 – Actual versus RSM values for Noise

	High Efficiency	Low Noise
Noise – Actual (dB)	69.39	68.12
Noise – RSM (dB)	69.44	68.10
% error	0.07%	0.04%

The predicted characteristic of the two rotor obtained from the Pareto Front are compared with the baseline in Fig. 12. The results confirm that all the geometries meet the requirements on the pressure rise at two duty points and High Efficiency design results in higher efficiency at low flow rate which is expected but the Low Noise design in fact results in a higher efficiency at high flow rates. The efficiency at high flow rate was not actually used as an objective in this study. But it is possible to use the same Response Surface to try and a obtain a different set of Pareto Front based on for example efficiency at high flow and low flow subject to some constraint on noise.

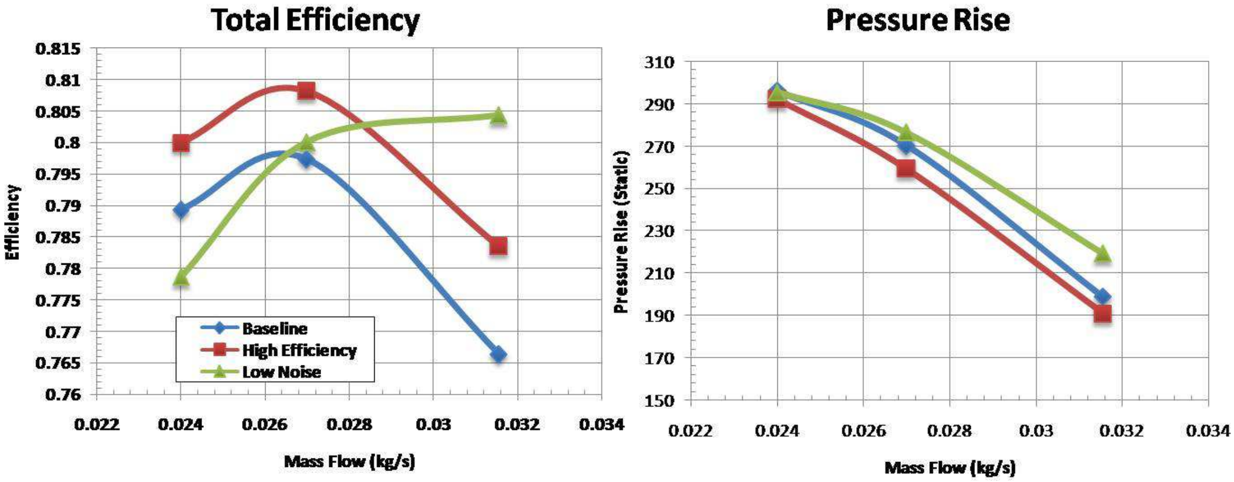

Figure 12: Characteristic for the baseline, high efficiency and low noise design

The details of the flow field in the 3 different designs are compared in Fig. 13 at low flow rate. The results indicate that in the High Efficiency design the stagnant region near the trailing edge suction surface is well suppressed.

a)

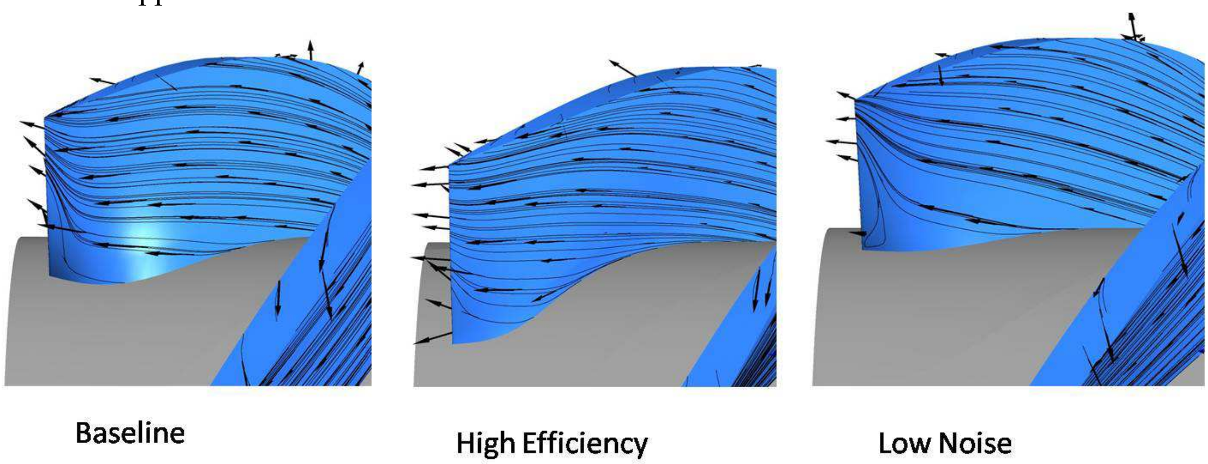

Figure 13: Secondary flows at trailing edge

CONCLUSIONS

A methodology was presented for design of fans in which 3D inverse design method is coupled with a multi-objective/multi-point automatic optimization strategy based on Design of Experiments, Response Surface Modelling and Multi-Objective Genetic Algorithm. The methodology was applied to the design of a generic CPU cooling fan with high rpm and relatively high required pressure rise. The fan had to meet specified performance at two duty points about 30% different in flow rate. The aim was to improve efficiency at low flow rate, reduce noise and maintain the required pressure rise at the two duty points. The noise prediction was obtained from Ffowcs-Williams Hawkins model using the blade surface pressure and blade geometry obtained directly from the 3D inverse design code. In total 7 design parameters, related to blade loading, spanwise$r\bar{V}_\theta$and stacking condition were used to parameterize the blade. The Design of Experiment method was used to create an experimental table consisting of 36 different geometries. All of these geometries were analysed in CFD at 3 different points and also their noise was predicted. The resulting response surface was found to be fairly accurate. MOGA was then run on the response surface to see the trade-off between the efficiency at low flow and the noise level subject to constraints on pressure rise at the two duty points. Two points on the Pareto front representing high efficiency and low noise were then selected for further study and validation.

Previous work using inverse design method has shown that the blade loading to improve a particular flow feature has generality and can be applied to other similar applications. So in fact this approach can be used as a means of rapidly developing new know-how in design of fans that meet difficult multi-point/multi-objective requirements.

BIBLIOGRAPHY

[1] J-H. Zhou, C-Z.Yang – *Design and Simulation of the CPU Fan and Heat Sinks***,** IEEE Transactions**,** Components and Packaging, Vol 31, pp. 890-904.**(2008)**

[2] C. M Jang, M. Furukawa, M. Inoue – *Analysis of Vortical Flow Field in a Propeller Fan by LDV Measurements and LES Part I:Three-Dimensional Vortical Flow Structures*, Transactions of the ASME, Journal of Fluids Engineering, Vol 123, No.4, pp. 748-754, **2001.**

[3] TURBOdesign1 - Advanced Design Technology Ltd, **2011**.

[4] H. Okamoto, M. Zangeneh, H. Watanabe, A. Goto – *Design of a box fan rotor using 3-D inverse design method*, IMechE International Conference on fans, 9-10 November **2004**, London.

[5] K-Y Lee, Y-S Choi, Y-L Kim, J-H Yun – *Design of axial fan using inverse design method*, Journal of Mechanical Science and Technology, vol. 22 pp. 1883-1888, **2008.**

[6] H. Okamoto, A. Goto, M. Furukawa – *Design Of A Propeller Fan Using 3-D Inverse Design Method And CFD For High Efficiency And Low Aerodynamic Noise.* ASME paper FEDSM2009-78454, **2009.**

[7] TURBOdesignOptima , Advanced Design Technology Ltd, 2011.

[8] J. E. Ffowcs Williams, D. L. Hawkings – *Sound generation by turbulence and surfaces in arbitrary motion*. Phil. Trans. Ryo. Soc., A264, **1969**

[9] R. H. Myers – *Response Surface Methodology –Current Status and Future Direction*, Journal of Quality Technology, **31**, No.1, pp. 30-44, **1999.**

[10] Taguchi, G., 1976, *Design of Experiment*, Maruzen, Tokyo

[11] K Deb, A Pratap, S Agarwal, T Meyarivan – *A fast and elitist multiobjective genetic algorithm: NSGA-II*, Evolutionary Computation, Vol 6, pp. 182-197, **2002**.

[12] M. Zangeneh – *A 3D Design Method for Radial and Mixed-Flow Turbomachinery Blades*, Journal of Numerical Methods in Fluids, **13**, pp. 599-624, **1991.**

[13] A. Tadamasa, M. Zangeneh – *Numerical Prediction of Wind Turbine Noise*, Renewable Energy, Vol. 36, pp. 1902-1912, **2011.**